Contents lists available at ScienceDirect

Thin Solid Films

journal homepage: www.elsevier.com

Ordered and disordered evolution of the pore mesostructure in hybrid silica anti-reflective films obtained by one-pot self-assembly method

Mohamed N. Ghazzal,*[,1] Damien P. Debecker, Eric M. Gaigneaux

Institute of Condensed Matter and Nanoscience, Molecules, Solids and Reactivity (IMCN/MOST), Université catholique de Louvain, Croix du Sud 2/L7.05.17, 1348 Louvain-La-Neuve, Belgium

ARTICLE INFO

Article history:
Received 11 November 2015
Received in revised form 23 March 2016
Accepted 11 May 2016
Available online xxx

Keywords:
Hybrid film
MTES/TEOS
Mesoporous
Inorganic-organic
Order-disorder
Silica
Anti-reflective

ABSTRACT

Hybrid mesoporous silica films were prepared in acid-catalysed medium using a one-pot self-assembly method. A gradual content of methyl groups was introduced into the inorganic framework by co-condensation of tetraethyl orthosilicate and methyltriethoxysilane. To better understand how the ordered and disordered transition occurs in mesoporous hybrid organosilica sytem as function of the MTES molar ratio in the starting solution, textural, chemical and optical properties of the films were studied by transmission electronic microscopy (TEM), grazing-incident small angle X-ray scattering (GISAXS), transmission Fourier transformed infrared (FTIR) and UV–visible spectroscopy. Increasing the loading of the incorporated organic groups (up to 40% in the starting solution) led simultaneously to a disorganization of the pore mesostructure and a reduction in the pore diameter. Concomitantly, a disordered domain of the silica rings in the walls was observed, which created bond strains in the silica wall contributing also to the disorganization of the pore mesostructure. Furthermore, an optimal MTES content was identified in order to obtain antireflection coatings, exhibiting low reflection in the visible range.

1. Introduction

One-pot co-condensation of hybrid precursors in solution is a useful method to incorporate organic functional groups into a silica inorganic network, yielding specific pore surface properties such as hydrophobicity, optical, catalytic and electronic activities. Porous silica materials with well distributed mesophase can be obtained by the evaporation-induced self-assembly method (EISA) using a precursor solution containing a template [1,2]. Pyrolysis is usually used to destroy the template revealing a mesostructured void in the silica material. EISA have received great interest due to its simplicity to produce a wide range of mesoporous metal oxides [3,4]. Currently, this method also offers the best way to homogenously disperse organic function within the silica oxide matrix or at its surface [5] and to control the stoichiometry of chemical pending groups [6]. Hybrid mesoporous material showed a wide range of potential applications in catalysis [7], sensing [8,9], energy [10] optics [11] *etc*. Mesostructured organosilica films obtained *via* the co-condensation of self-assembly hybrid precursors in solution of methyltriethoxysilane (MTES)-tetraethyl orthosilicate (TEOS) were widely studied [12,13], mainly because of the relative stability of the methyl group during a calcination up to 400 °C [5].

Converting the inorganic framework to hybrid through the incorporation of an organic functional group can lower the dielectric constant of the film [14]. Although variable mesophases have been reported for hybrid systems [12,13,14], a systematic disordering of the mesostructure occurs when the molar ratio of the MTES in the starting solution increases. A threshold was often reported when pendant organic functionalities are incorporated and the ordering of the mesopore is generally completely lost above 20 mol% MTES in the starting solution [2]. Strong efforts have been made to produce highly ordered materials with the organic functionality required for device applications. The synthesis conditions were studied and designed to control the reactivity of the silica oligomer and to reduce the perturbation due to the modification of the surface energy at the organic-groups/template interface [12]. Electro-assisted deposition has been also applied as useful process to build hybrid system by co-condensation of alkoxysilane and organosilane [15]. Recently, electro-assisted method shows the ability to reach high functionalization level of (3-azidopropyl)trimethoxysilane up to 40% mol. of the starting solution [16].

While most of the research has been focused to make the mesostructure more stable, few studies were dedicated to better understand the disorganization of the mesostructure for such kind of hybrid systems. Several parameters are the potential causes of the loss of order. They are generally related to the synthesis conditions. Jung et al. [14] suggested that the disordering of the mesoporous organosilica films at high MTES/TEOS molar ratio is caused by a lengthy sol aging time. A longer organic side chain was also reported as detrimental to preserving the mesostructure [14].

* Corresponding author.
Email address: g_nawfel@yahoo.fr (M.N. Ghazzal)
[1] Present Address: Université de Mons, Laboratoire de Physique des Surfaces et Interfaces Campus Plaine de Nimy, Bâtiment 4 19, Avenue Victor Maistriau 7000 Mons, Belgique.

http://dx.doi.org/10.1016/j.tsf.2016.05.018
0040-6090/

In the present study, mesoporous methylated organosilicate thin films were synthesized by one-pot co-condensation of MTES and TEOS precursor with a rapid solvent evaporation *via* spin-coating. The films mesostructure as well as the hybrid wall chemical composition were investigated before and after calcination. The solvent evaporation and the kinetics of the condensation of the system which occurred simultaneously are discussed, in order to explain the disorganization mechanism of the mesostructure. Furthermore, optical properties of the films were evaluated by UV–visible spectroscopy as they are designed to be antireflective coating.

2. Experimental set up

Hybrid silica films were obtained by mixing TEOS with different proportions of MTES under acidic conditions. Sol synthesis and films elaboration were prepared by adapting the procedure described elsewhere [5]. Hybrid silica films were obtained using one-pot co-condensation of two precursors ($Si(OC_2H_5)_4$, TEOS, Aldrich and $CH_3Si(OC_2H_5)_3$, MTES, Aldrich) with different proportions in the presence of an adequate amount of water (Milli Q, 18 Ω), in ethanol (absolute grade). The pH was adjusted at $_amp_$lt; 2 with hydrochloric acid (Aldrich, 37%). The molar ratio of MTES/(MTES + TEOS) was varied from 0 to 0.8. Final molar ratios after the template addition (triblock copolymer Pluronic P68; ~ 8.400; $EO_{80}PO_{30}EO_{80}$) were MTES/TEOS/H_2O/EtOH/P68 = *x*:*y*:10:20:0.01. The coatings were obtained *via* spin-coating the so prepared hybrid solutions at 5000 rpm during 30 s on the substrates. The substrates were previously cleaned under sonication by detergent, acetone, ethanol and finally by MilliQ water (18 Ω). The films were submitted to a drying process during 6 h at 70 °C, and then the template was destroyed by heating the samples in air at 400 °C for 2 h using a heating ramp of 1 °C·min^{-1}.

3. Thin film characterization

Transmission electron microscopy (TEM) images were obtained with a JEOL 2000FX instruments, working under an acceleration voltage of 200 kV. The samples were scratched off from the substrate and dispersed in ethanol. A droplet of the suspension was deposited on the cooper grid and dried before analysis.

The mesostructure of the mesoporous hybrid silica films before and after calcination was carefully checked by small-angle X-ray scattering at grazing incidence of 0.2°. The GISAX*S*-Rigaku S-max 3000 facility was equipped with a microfocus source λ = 0.154 nm and a 2D Gabriel type detector. The distance between samples and the detector was fixed at 1494 mm. The transmitted and specular reflected beams were masked by a vertical beam-stop.

Fourier transform infrared (FTIR) spectra (200 scans were averaged with a resolution of 4 cm^{-1}) were recorded using Bruker EQUINOX 55 spectrometer in static air in the range of 4000 cm^{-1} – 400 cm^{-1}. The spectra of the hybrid silica thin films were obtained by coating the KBr pellets by 0.1 ml of precursor solutions, which enables specific recording the IR region meanwhile the soda lime slide was not transparent to. Maintaining the same amount deposited in KBr pellets enable to have a quite-quantitative comparison of the infrared spectra. The spectrum of a non-coated KBr pellet was used as the background. Measurements were performed for the thermally-treated samples at different temperatures (70 °C in air for 6 h and 400 °C in air for 2 h) and following identical successive and variable condensation–consolidation temperatures as described above for the films.

Static water contact angles (Θ) were measured at ambient temperature and humidity using the sessile drop method and image analysis of the drop profile. The instrument, consisting of a CCD camera and an image analysis processor, was purchased from Electronisch Ontwerpbureau De Boer (The Netherlands). The water (Milli-Q, Millipore, Molsheim, France) droplet volume was 3 μl and the contact angle was measured 5 s after the drop deposit onto the sample. For each sample, the reported value consisted of the average of the results obtained using at least 5 droplets.

Transmittance measurements in the range of 300–800 nm were carried out using a UV–Visible spectrophotometer (Cary5E) at a normal angle of incidence.

The thickness of the film is measured using atmospheric ellipsometric porosimetry (A-EP) performed with equipment from Sopra (Model GES-5E, A-EP, Sopra, Paris, France) using the software package "WinElli2". More details concerning the procedure used can be found elsewhere [9].

4. Results and discussion

4.1. TEM analysis

The ordered and disordered evolution of the mesostructured for hybrid silica films obtained by self-assembly method and after calcination at 400 °C was first analyzed as function of the molar ratio of MTES by TEM (Fig. 1). The mesoporous silica thin film prepared using solely TEOS precursor (Fig. 1.a) shows a well-organized and defect-free mesostructure. From the TEM images, it is challenging to unambiguously distinguish whether the bright circular features were attributable to cylindrical or spherical pores. In the image taken in plane view, the spheres appear overlapped such as forming cylinders. This confusion results from the observation angle, which was previously observed for Body-centered cubic mesostructure [17,18]. Thus, the identification of the mesophase structure is not straightforward. GISAXS technique was, therefore, effectively applied to achieve a better identification of the organized mesophases (see below). The hybrid silica film with a 10% of MTES molar ratio in the starting sol shows the same organization of the pore over a large area (Fig. 1.b). However, the periodicity of the mesopore was destroyed at MTES molar ratios higher than 10%. Worm-like structure appeared as a result of randomly distributed micelles for molar ratio of MTES ranging between 25% (Fig. 1.c) and 40% in starting sol (Fig. 1.d). Beside a disorganization of the mesostructure, an increase in loading of the incorporated organic groups lead to a reduction in the pore diameter. A nonporous hybrid silica film was obtained when the MTES molar ratio exceeded 60% in the starting sol (Fig. 1.e and .f).

4.2. GISAXS analysis

GISAXS patterns of the films before and after calcination are presented in Fig. 2. Both patterns exhibit two kinds of repartition for the X-ray diffuse scattering.

Firstly, for MTES contents of 0 and 10%, the Bragg diffraction spots are clearly observed. This confirms that the pores are highly organized and structured, and drying steps did not affect the crystallization. This pattern can be indexed as the Body-Centered Cubic (BCC) $Im\bar{3}m$ unit cell in, showing only reflections [011] perpendicular to the plane. Cell parameter "*a*" is of 8.53 nm and 8.36 nm for non-calcined 0 and 10% of MTES molar ratio, respectively. The films retain their ordered mesostructure up to 400 °C. However, the unit cell parameter *a* contracts to 8.3 nm and 8.1 nm after the calcination, as indicated from GISAXS patterns. The intensity of the Bragg diffraction spots before calcination is lower compared to that obtained after calcination, which is due to the lower contrast of electron density between the pores filled by the template and the silica matrix. The films are in-

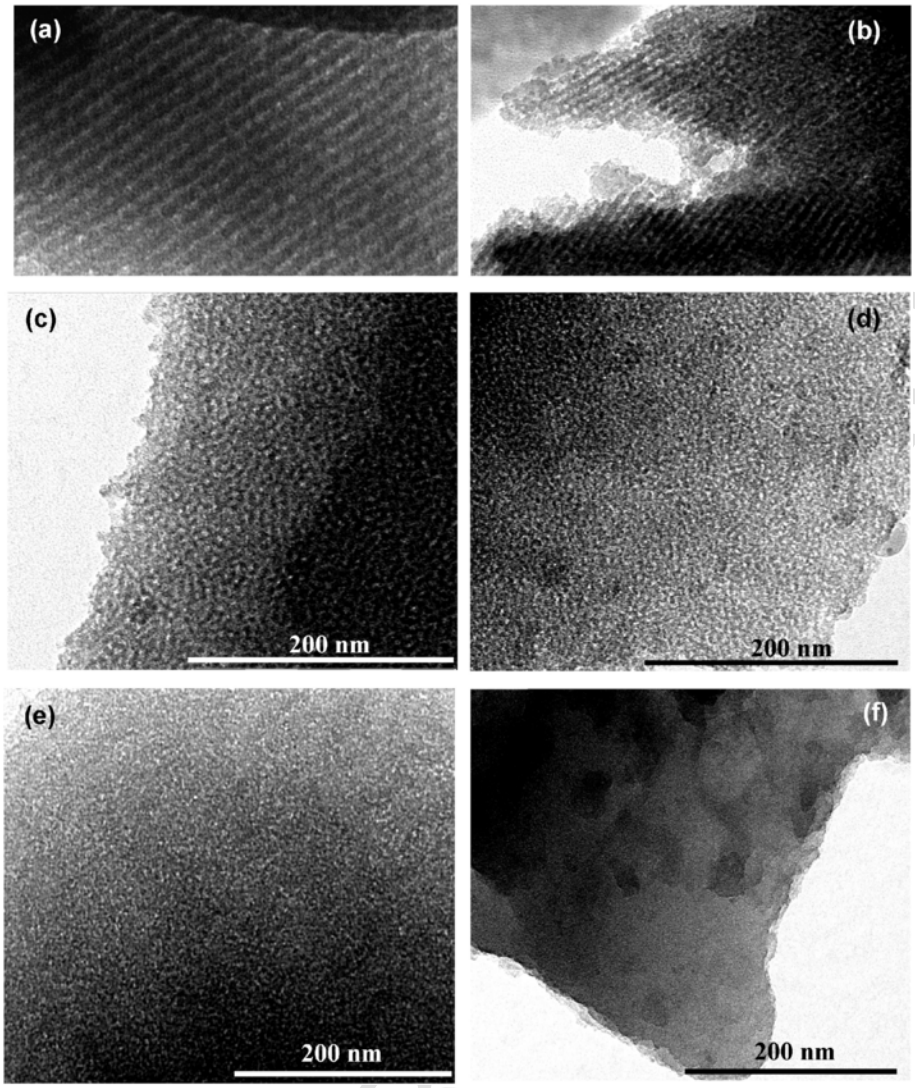

Fig. 1. TEM images of scratched samples at variable molar ratio of MTES precursor, (a) 0, (b) 0.1, (c) 0.25, (d) 0.4, (e) 0.6, (f) 0.8.

fluenced by a deformation which occurred in a direction perpendicular to the substrate. Indeed, the spots position of q_z are localized at a higher position after the heating, whereas they are at the same position in q_y-position. This confirms that the thermal treatment has no effect on the periodic structure in the film plane parallel to the substrate. However, a contraction along a direction perpendicular to the film plane is observed. The deformation results from the presence of a strain in the mesostructured silica films. The drying and thermal treatments are complex processes in traditional sol-gel films preparation. The silica pore wall shrinks during these two processes. The shrinkage of the film, which can only occur in the direction (z) normal to the substrate (uniaxial shrinkage), arises because the film is constrained to the substrate; this shrinkage thus produces a tensile stress in the films and a compressive stress in the substrate [19].

Secondly, at higher molar ratios of MTES in the starting sol (25% and 40%), the Bragg diffraction spots disappear leaving a place to a faint ellipsoidal circle. This corresponds to mesostructured pores, but with random orientation relatively to the surface [20]. The results match very well with the wormlike structure identified by TEM images (Fig. 1c and d). At higher MTES molar ratio, GISAXS patterns do not show any diffraction, confirming the destruction of the mesostructure.

In our study, no major difference in the mesopore organization was observed *via* GISAXS before and after calcination at high temperature. These results suggest that the pore organization is already achieved during the spin-coating process and the pyrolysis had no effect on the pore organization. The transition of ordered to disordered of mesoporous organosilica films made by the EISA method is complex and is driven by several parameters such as the aging of the silica sol [13], the nature of the silicon alkoxide precursor used [14], and the experimental conditions of the coating [21].

In order to understand the disorganization phenomenon of the mesophase, it is important to look further in the micelle formation and the self-assembly process. The concentration of surfactant used in this study is above the critical micelle concentration (cmc) and the presence of other molecules such as MTES decreased the cmc even further. The micelles formation takes place during the spin-coating process and more precisely during the solvent evaporation. The solvent evaporation increases the surfactant concentration and the cmc is reached [21]. Thus, the micelle aggregation induces the apparition of a liquid crystalline phase. In the best condition, micelles stack in or-

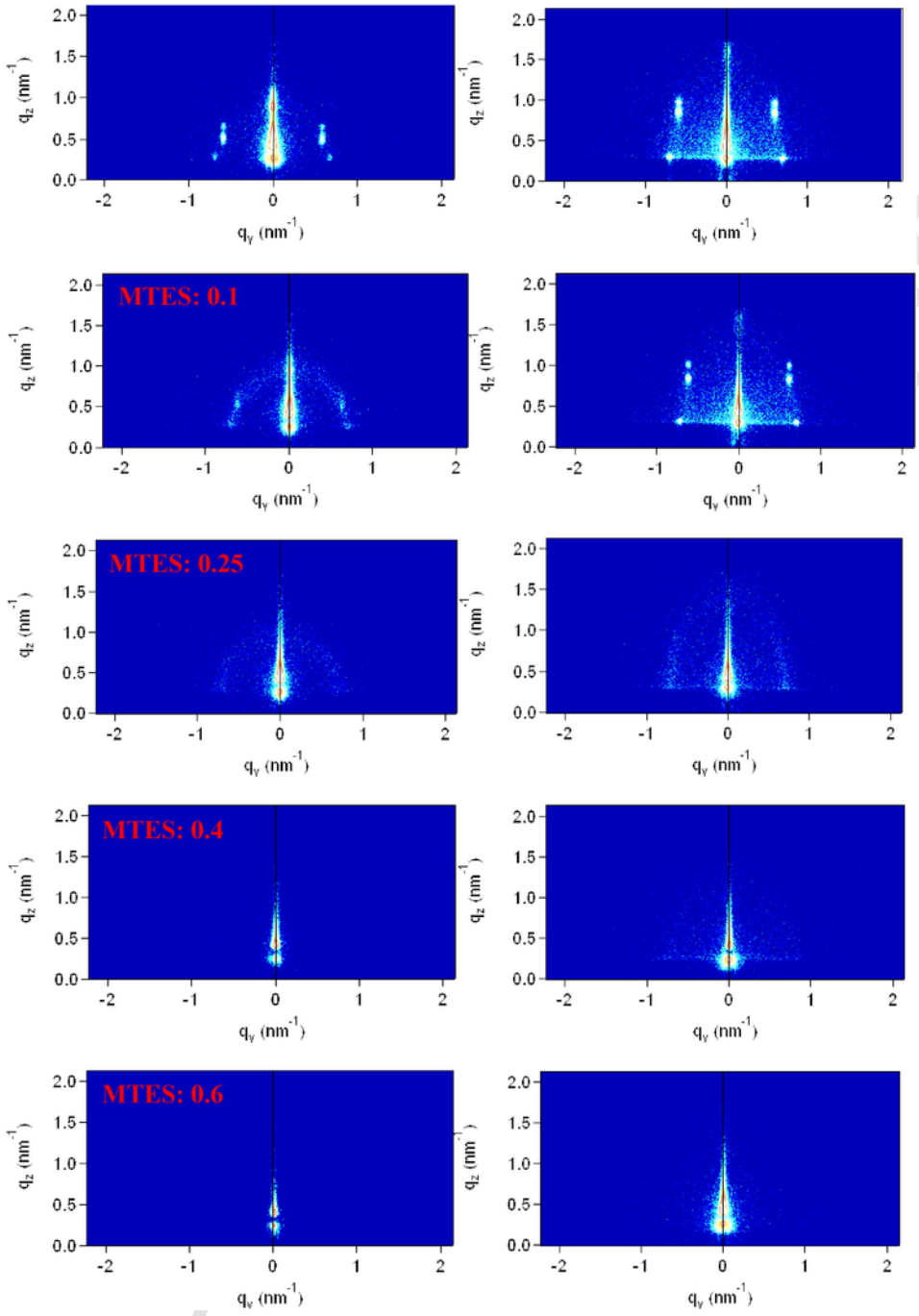

Fig. 2. GISAXS patterns for the hybrid silica films with variable MTES ratio before (left) and after (right) calcination at 400 °C.

dered structures and the inorganic skeleton surround the organic liquid-crystalline phase. The mesostruture is achieved and commonly results from a balance of the competition of inorganic polycondensation and the ability of the surfactant to form micelles [20].

Falcaro et al. [13] highlighted the role of methyl groups present in the silica sol to help the self-organization of the inorganic oligomers around the micelles for low MTES molar ratio in the starting sol. They reported that introducing methyl groups affected significantly the micelle/silica interface and the kinetics of the reactions of the species involved in EISA. The presence of CH_3 in the silica oligomers reduces the interactions between the silica and the template, while at the same time the kinetic of polycondensation also becomes smaller. In these conditions, the organization of the micelles is not delayed by a more condensed inorganic network, and very high organization is reached. Since the MTES molar ratio was the only parameter varied, we can reasonably assume that the partial substitution of hydroxyl groups by methyl groups reduces the polycondensation kinetics of the inorganic silica oligomers. This explains the highly mesostructured film obtained until a molar ratio up to 10% (MTES molar ratio = 0–10%; Fig. 3.a).

However, the kinetic of polycondensation of the silica oligomers is not anymore the dominant parameter that drives the self-organization of the micelles, since a wormlike structure appeared for higher concentration of CH_3 groups. Moreover, a complete disorganization

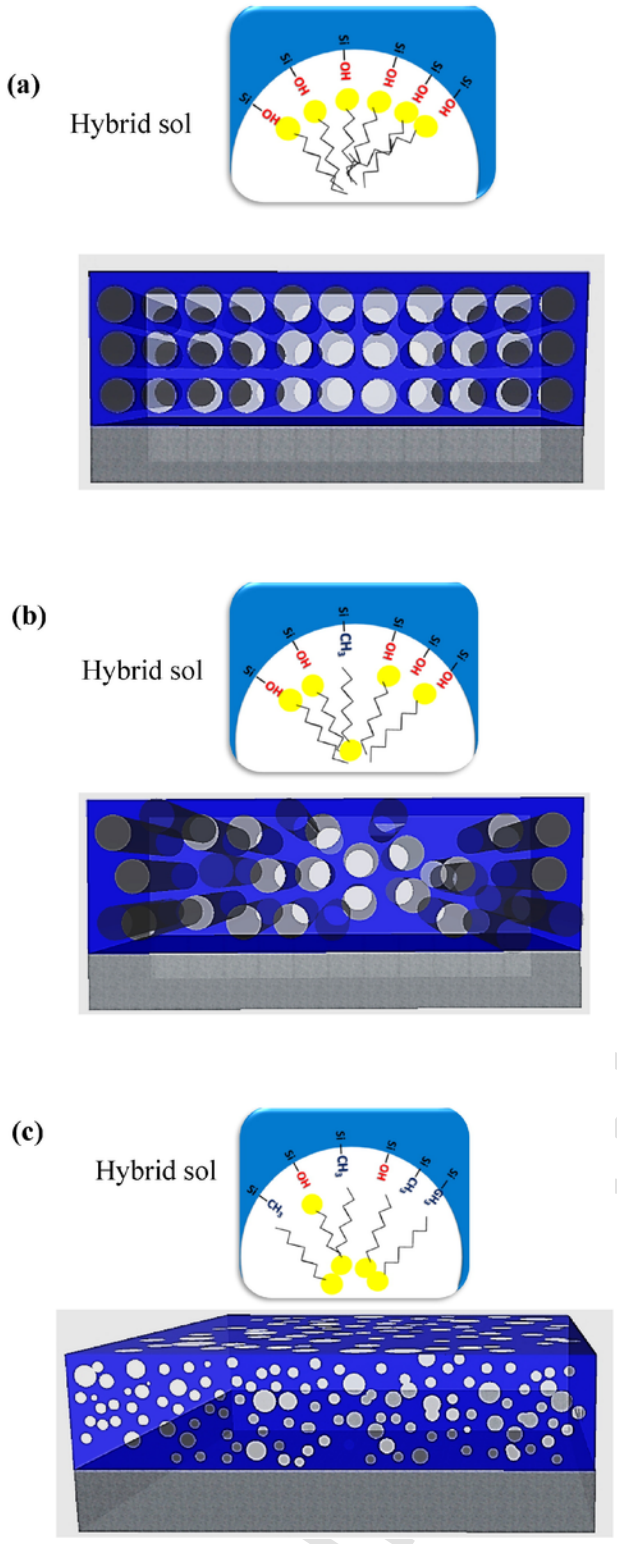

Fig. 3. Evolution of the mesostructure of hybrid silica film by increasing MTES content.

of the pore is achieved for 25% and 40% (MTES molar ratio = 25%–40%; Fig. 3.b). The interaction between the methylated silica oligomers and the template became the limiting parameter. The interaction of the silica oligomers and the surfactant is considerably disturbed. The hydrolysis degree of the inorganic species (many research groups have considered that Si—OH groups are roughly equivalent to water [22]) at the surface has been proved to be an important parameter which contribute efficiently to enhance the formation of ordered micelle arrays, and control the interactions between the template and the inorganic network [23]. Raising the methyl pendent groups by increasing the MTES ratio in the starting sol disrupted the insertion of the water (Si—OH) between the polar head of the micelles and the inorganic framework. The fluidity needed which allows the micelle the required mobility to organize themselves was then reduced. The organization of the template in crystalline mesophase is prevented. In addition to the perturbation due to the order transition, the pore size was reduced. This can be explained by the fact that lower numbers of template molecules were forming the micelles. The reduced fraction of silanol groups disturbed the previously established "Template/Precursor/water (Si—OH)" equilibrium. The micelle formation was completely lost for higher molar ratio of MTES and the sol contained separate template molecules (Fig. 3.c). In such case, the films obtained after calcination appeared with low porosity.

4.3. FTIR analysis

FTIR transmittance spectra, collected in air, for each hybrid silica sample treated at increasing temperatures (70, 150, 200, 300 and 400 °C) are shown in Fig. 4. The main objective of this characterization was to uncover important information for several features attributed to hybrid silica structure (cyclic species), the surfactant, methyl groups and residual water. However, we did not aim to better understand the condensation kinetics process occurring when the solvent evaporation starts. The cyclic species in silica precursor solutions has been well described by ^{29}Si nuclear magnetic resonance (NMR) experiments [24]. Cyclic species, especially those of lower dimensions such as twofold, threefold, and fourfold rings are found to be thermodynamically unstable, since the order is easily lost during thermal treatment. These vibrations mode attributed to the silica cyclic species can be taken as the silica fingerprint to identify the modification of the structure. However, to assess the presence of these structures in thin films is very difficult to perform. The particular processing conditions that are used for self-assembly of silica films (low pH) can produce the formation of different ordered units of rings. The techniques that can give a direct *in situ* indication of the presence of silica rings are FTIR or Raman [25] which are quite difficult to perform on thin films (Raman). In our study, we used coated KBr pellets with the hybrid sols as an effective solution to study the silica cyclic species by FTIR. FTIR spectroscopy was previously performed for silica inorganic mesoporous films [12,20]. Although the authors provide data about the polycondensation kinetics, only the roles played by the surfactant or the temperature for inorganic silica films were discussed. The surfactant-containing system was found to be the cause of the scaling down of the solvent evaporation rate, whereas the temperature affects the structure of the silica structure. In the present study, we focused on the disordering occurred on the cyclic species of the hybrid silica structure, a region from 400 to 1400 cm^{-1}, as function of a rising temperature and when the ratio of MTES/TEOS is varied.

With solely TEOS as precursor (Fig. 4.a), the band assigned to the residual surfactant (1352 cm^{-1} and 794 cm^{-1}) decreased with temperature, and after a 400 °C thermal treatment this band disappeared completely. The intensity of the Si − OH stretching band around 950 cm^{-1} was reduced when the films were calcined, and the same was observed when the molar ratio of the MTES in the starting sol

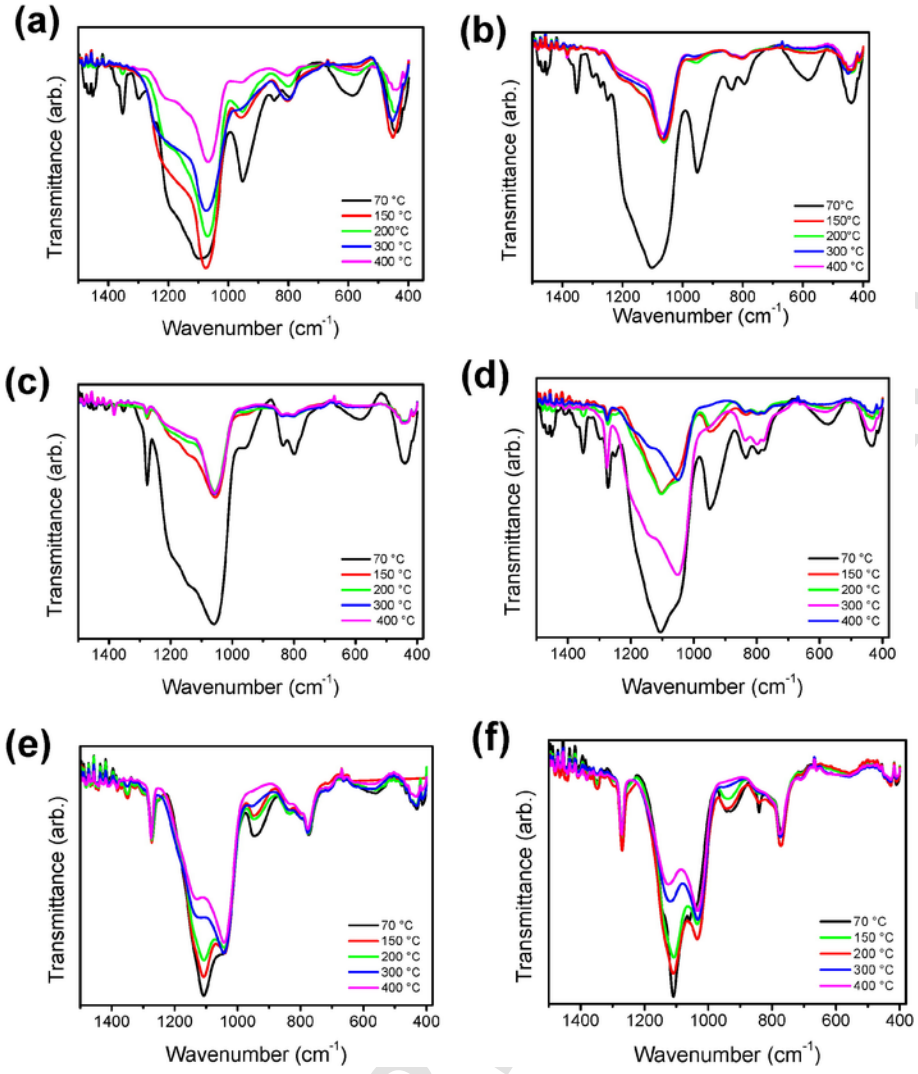

Fig. 4. FTIR transmittance spectra of hybrid silica films coated KBr with MTES ratio of (a) 0, (b) 0.1, (c) 0.25, (d) 0.4, (e) 0.6, (f) 0.8 calcined at increasing temperatures (from 70 °C to 400 °C).

was increased (Fig. 4.b–f). Increasing MTES molar ratio induces a major spectral change. The incorporation of a methyl group in the silica network resulted in the appearance of peaks (1276 cm^{-1} and 790 cm^{-1}) corresponding to the vibration mode $Si-CH_3$ (Fig. 4.b–f). The first was assigned to the C − H deformation modes and the second to the Si—C stretching modes [9]. The methyl group showed great stability even when calcined at high temperature (400 °C during 2 h). A good correlation can be found between the intensity of this band and the MTES content, suggesting a higher functionalization level.

The peaks around 1070, 800 and 440 cm^{-1}, characteristic of the Si—O—Si [24] bonds vibration modes, were detected for samples with low MTES ratio or when solely TEOS was used. Antisymmetric stretching (third transverse optical; TO_3) mode with high intensity was located at the frequency mode of 1070 cm^{-1}. The symmetric stretching (second transverse optical; TO_2 mode) revealed by a weak peak at 800 cm^{-1} is assigned to Si—O—Si bonds. Near 440 cm^{-1}, the peak is assigned to the transverse optical rocking motions (TO_1 mode). The transverse optical asymmetric stretching modes appeared with a shoulder at high frequencies. The nature of this bond is very complex and the attribution of its vibrational modes is yet unclear [24]. For a low MTES molar ratio ($_amp_$lt; 25%), the band at 1068 cm^{-1} and 1190 cm^{-1} could be assigned to the transversal optical (TO) vibration mode, whereas the 1140 cm^{-1} and the 1220 cm^{-1} to the longitudinal optical (LO) vibration mode of the Si—O—Si bonds [23]. The shoulder intensity decreased by heating the sample at higher temperature. Although the experiment enabled a qualitative comparison, the decrease of the peak intensity with rising temperatures provides important insights into the cyclic species composing the silica structure. The bands around 1220 cm^{-1} assigned to the three-membered cyclic species were thermodynamically instable and disappeared at 400 °C, while the band at 1140 cm^{-1} persisted, indicating the stability of the octameric silicon arrangement [25]. Increasing the MTES molar ratio ($_amp_$gt; 0.25) significantly enhanced the LO mode and thus the formation of four-membered cyclic species, as evidenced by the peak around 1109 cm^{-1} for the sample heated at 70 °C. The peak position shifted to higher wavenumber (from 1109 to 1130 cm^{-1}) when the calcination temperature exceeded 300 °C, whereas the peak at 1070 cm^{-1} assigned to the TO mode vibration of the Si—O—Si network shifted to lower wavenumbers. The shift of the TO mode is usually observed when the temperature increases and is correlated to increasing porosity during the solvent evaporation or the surfactant degradation [24]. Other shifts were also observed when comparing the FTIR transmittance of the films

isothermally-treated at 400 °C (Fig. 4). An intense broad band between 2900 and 3700 cm^{-1} was detected (Fig. 5.a). The large band was due to the vibration of O—H groups originating from the silanol groups and adsorbed water linked to the surface by hydrogen bonds. The band quickly disappeared when methyl group were introduced in the network by increasing the MTES content (Fig. 5.a). This correlated well with the increase of the intensity of the bands corresponding to the methyl groups incorporated into the films, as well as with the decrease of the Si—OH peak around 960 cm^{-1} (Fig. 5.b), demonstrating higher functionalization levels. Consequently, the surface of the films became more hydrophobic, which was confirmed by the static angle measurement (Fig. 5.c). Substituting the hydroxyl groups by methyl groups in the silica surface as well as in the pore surface, induced the formation of the small silica cyclic species in the surface (small silica rings) [26]. This was confirmed by the shift to lower wavenumber of the TO mode vibration of the Si—O—Si band (from 1076 to 1035 cm^{-1}), suggesting a strengthening of the silica network due to polycondensation [26]. Concomitantly to the observed shift, a distinct peak appeared at 1145 cm^{-1} for 0.4 MTES molar ratio; at higher molar ratios, the peak shifted to lower wavelengths.

The modification of these optical modes confirms the presence of a disordered domain of the silica structure. As prepared the silica structure showed an arrangement of its cyclic species in three-membered and octameric silicon. While the first arrangement disappeared by increasing the temperature, the second one remain stable. Furthermore, the formation of four-membered cyclic species was enhanced by substituting hydroxyl groups by methyl groups. Increasing methyl groups in the silica structure modified the Si—O—Si bond distance as well. This created bond strains in the silica pore wall which strongly influenced the mechanical properties leading to a disorganization of the pore mesostructure.

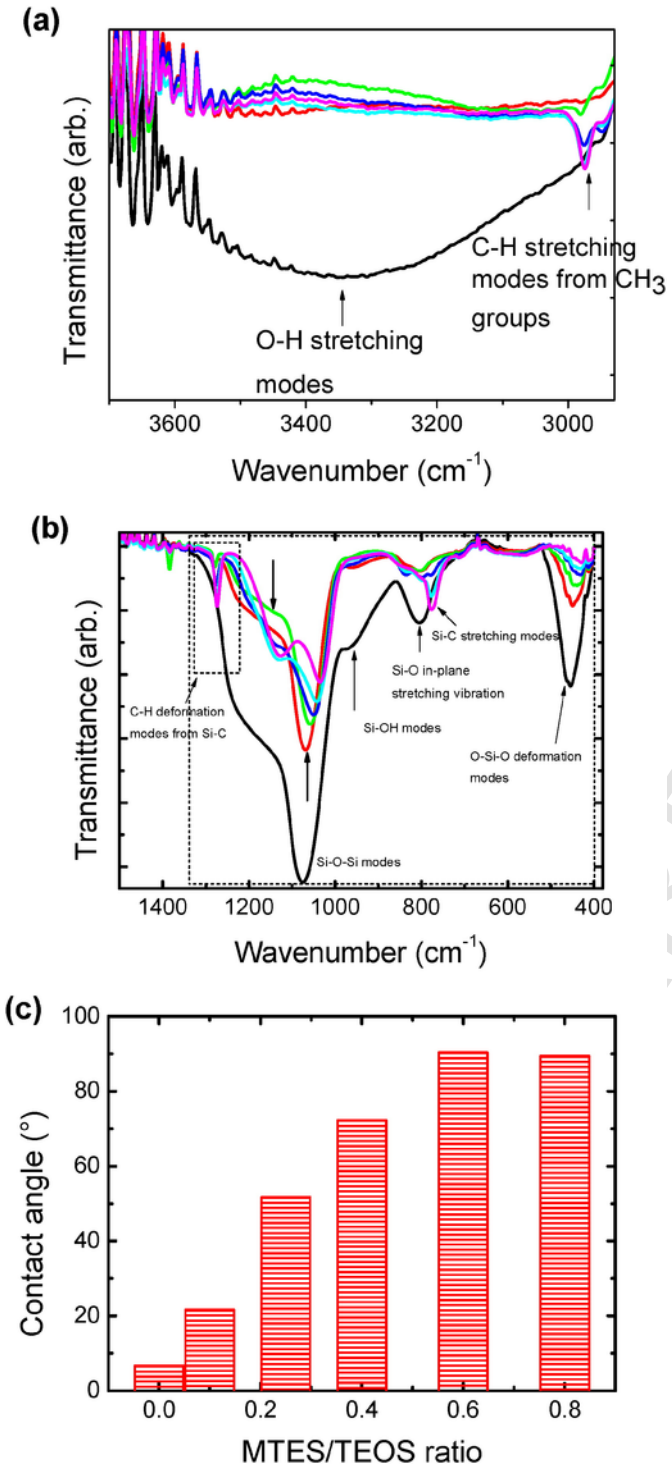

Fig. 5. (a) and (b) FTIR spectra of a hybrid silica layer with increasing MTES content treated at 400 °C, (c) Static water contact angle dependence on the MTES ratio.

4.4. Antireflection characteristics of hybrid films

Antireflection properties were assessed by UV–visible spectroscopy for different films for both single and double side coated glass. UV–vis transmittance of the glasses coated with the porous films was measured in the wavelength range from 400 to 800 cm^{-1}. The transmission spectra of coated glass are reported and compared to the spectrum of an uncoated glass in Fig. 6. It is obvious that the porous coating improved the transmittance of the glass, even if only one side is coated. The transmittance reached 93.94% when one side was coated and 96.62% when both sides were coated. The wavelength at the maximum transmittance (λ_{max}) was red-shifted (Fig. 6.a). This could be correlated to a change of the film thicknesses since λ_{max} has a linear dependence on the refractive index and the thickness as well; $\lambda_{max} = 4dn$ (n: refractive index and d: film thickness) [27]. Indeed, the thickness of the films was assessed using ellipsometric spectroscopy (Table 1). Despite the fact that the polycondensation of the silica films is affected by the MTES (d = 0.955 g/ml) ratio, the viscosity of the starting sol has expected to increase since the density of the TEOS precursor is lower (d = 0.895 g/ml). However, no correlation could be observed between the thickness measured and the content of MTES precursor, suggesting that the effect of adding the MTES precursor on the viscosity is low. As we can see from the Table 1, the thickness of the films varies from 93 to 189 nm. The films obtained using the ratio 0, 10%, 25%, 60% and 80% show a comparable thickness. The large variation concern the film obtained using 40% MTES ratio. These variations could be due to the coating process. The organic group incorporated into the films is detrimental for the optical properties of the films, the maximum transmittance of the substrate decreased. This result could be related to the evolution of the pore order and then to the densification of the hybrid film when the film become non porous at higher methyl group content. Not only increasing the molar ratio of MTES causes the perturbation of the pore mesostructure (as shown above), it also inhibits the pore formation evidenced by TEM analysis (MTES/TEOS ra-

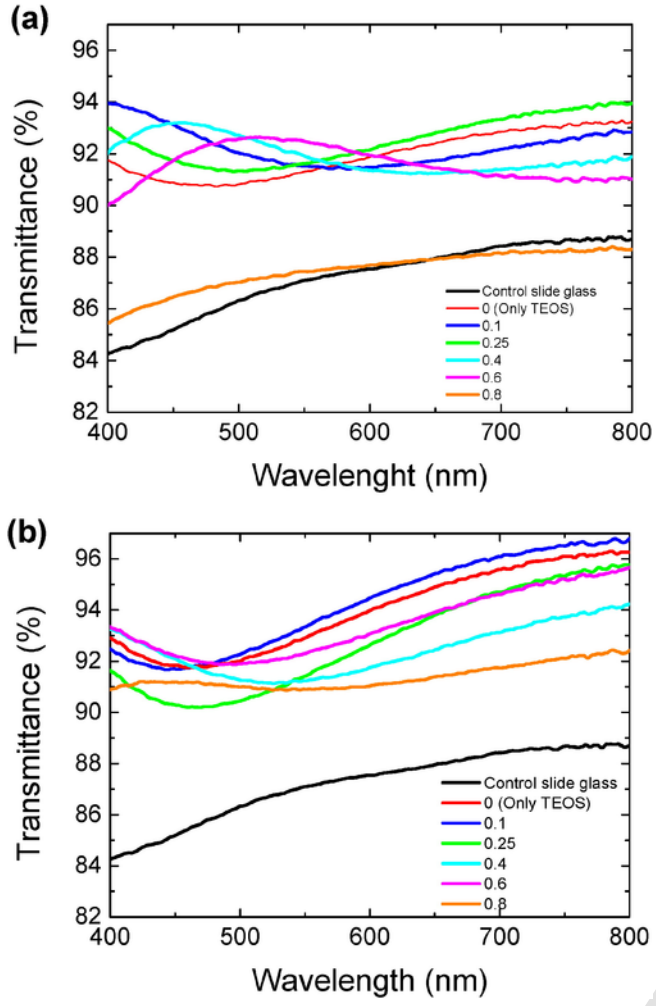

Fig. 6. UV–visible transmission analysis at 90° incident angle of (a) the single and (b) both side coated glass microscope slide substrate for variable hybrid system.

Table 1
Films thicknesses as function of increasing the molar ratio of MTES in the starting sol.

MTES molar ratio	0	10%	25%	40%	60%	80%
Films thicknesses	97 nm	130 nm	93 nm	189 nm	127 nm	119 nm

tio $_amp_$gt; 60%). The reduction of the pore size and the volume of void could lead to an increase of the films refractive index. At higher MTES molar ratio, the film was non porous and the transmittance was significantly affected. However, the transmittance remained higher than that observed for the non-coated glass. The refractive index of the organosilica layer was lower than the glass itself. The organosilica film obtained by substituting the silanol groups by methyl groups is reported to have low refractive index. The shrinkage is less important in the organosilica framework when the Si—O—Si linkage is reduced in favor of Si—CH_3, and a porous phase is formed around the pendant methyl groups since these cannot condense [5].

5. Conclusion

Functionalization of silica framework by methyl groups with a mesostructured pore was successfully obtained using mixtures of MTES and TEOS precursors. The ordered mesophase was preserved for a MTES molar ratio between 0 and 10% but was clearly affected at higher MTES content. The BCC mesostructure obtained at low METS content was destroyed step by step as function of increasing the MTES content: the pores show a wormlike structure at intermediate MTES molar ratio and finally with no organization at all at high MTES molar ratio. However, the hybrid silica films remain porous with a MTES molar ratio up to 60%. The wormlike structure results from the reduced interactions between the silica and the template due to the introduced methyl groups. Adding the methyl group in the silica wall pore was found to induce a disordered domain of the silica structure. An arrangement of the silica cyclic species in three-membered and octameric silicon was observed. While the first arrangement disappeared by increasing the temperature, the second one remain stable. Furthermore, the formation of four-membered cyclic species was enhanced by substituting hydroxyl groups by methyl groups. Increasing methyl groups in the silica structure modified the Si—O—Si bond distance as well. This created bond strains in the silica pore wall which strongly influenced the mechanical properties leading to a disorganization of the pore mesostructure. This creates a bond strains in the silica pore wall that influence the mechanical properties playing probably a key role for the disorganization of the pore mesostructure. These modifications also impacted the antireflective performance of the films: raising the organic group incorporated by adding the MTES precursor decreased the transmittance maximum of the substrate.

Acknowledgment

The authors thank C. Sanchez (UPMC) for providing access to the GISAXS facilities and M. Selmane for his help with the measurements.

References

[1] C.J. Brinker, Y. Lu, A. Sellinger, H. Fan, Adv. Mater. 11 (1999) 579–585.
[2] D. Grosso, C. Boissière, B. Smarsly, T. Brezesinski, N. Pinna, P.A. Albouy, H. Amenitsch, M. Antonietti, C. Sanchez, Nat. Mater. 3 (2004) 787–792.
[3] B. Eckhardt, E. Ortel, D. Bernsmeier, J. Polte, P. Strasser, U. Vainio, F. Emmerling, R. Kraehnert, Chem. Mater. 25 (2013) 2749–2758.
[4] L. Guo, H. Hagiwara, S. Ida, T. Daio, T. Ishihara, ACS Appl. Mater. Interfaces 5 (2013) 11080–11086.
[5] F. Cagnol, D. Grosso, C. Sanchez, Chem. Commun. (2004) 1742–1743.
[6] H.Y. Fan, Y.F. Lu, A. Stump, S.T. Reed, T. Baer, R. Schunk, V. Perez-Luna, P.G. Lopez, C.J. Brinker, Nature 405 (2000) 56–60.
[7] V. Hornebecq, Y. Mastai, M. Antonietti, S. Polarz, Chem. Mater. 15 (2003) 3586–3593.
[8] X. Wan, D. Wang, S. Liu, Langmuir 26 (2010) 15574–15579.
[9] M.N. Ghazzal, M. Joseph, H. Kebaili, J. De Coninck, E.M. Gaigneaux, J. Mater. Chem. 22 (2012) 22526–22532.
[10] T.-Y. Ma, Y.-S. Wei, T.-Z. Ren, L. Liu, Q. Guo, Z.-Y. Yuan, ACS Appl. Mater. Interfaces 2 (2010) 3563–3571.
[11] A.R. Balkenende, F.K. De Theije, J.C.K. Kriege, Adv. Mater. 15 (2003) 139–143.
[12] M. Matheron, A. Bourgeois, A. Brunet-Bruneau, P.-A. Albouy, J. Biteau, T. Gacoin, J.-P. Boilot, J. Mater. Chem. 15 (2005) 4741–4745.
[13] P. Falcaro, S. Costacurta, G. Mattei, H. Amenitsch, A. Marcelli, M.C. Guidi, M. Piccinini, A. Nucara, L. Malfatti, T. Kidchob, P. Innocenzi, J. Am. Chem. Soc. 127 (2005) 3838–3846.
[14] S.-B. Jung, T.-J. Ha, H.-H. Park, J. Colloid Interface Sci. 320 (2008) 527–534.
[15] Y. Guillemin, M. Etienne, E. Aubert, A. Walcarius, J. Mater. Chem. 20 (2010) 6799–6807.
[16] N. Vila, J. Ghanbaja, E. Aubert, A. Walcarius, Angew. Chem. Int. Ed. 53 (2014) 2945–2950.
[17] K. Yu, B. Smarsly, C.J. Brinker, Adv. Funct. Mater. 13 (2003) 47–52.
[18] X. Wu, K. Yu, J.C. Brinker, J. Ripmeester, Langmuir 19 (2003) 7282–7288.
[19] X. Wu, K. Yu, C.J. Brinker, J. Ripmeester, Langmuir 19 (2003) 7289–7294.
[20] D.A. Doshi, A. Gibaud, V. Goletto, M. Lu, H. Gerung, B. Ocko, M.S. Han, J.C. Brinker, J. Am. Chem. Soc. 125 (2003) (11646-11645).
[21] E.L. Crepaldi, G.J.d.A.A. Soler-Illia, D. Grosso, F. Cagnol, F. Ribot, C. Sanchez, J. Am. Chem. Soc. 125 (2003) 9770–9786.
[22] P. Innocenzi, P. Falcaro, D. Grosso, F. Babonneau, J. Phys. Chem. B 107 (2003) 4711–4717.

[23] H. Cho, A.R. Felmy, R. Craciun, J.P. Keenum, N. Shah, D. Dixon, J. Am. Chem. Soc. 128 (2006) 2324–2335.
[24] P. Innocenzi, J. Non-Cryst. 316 (2003) 309–3019.
[25] A. Fidalgo, L.M. Ilharco, J. Non-Cryst. Solids 283 (2001) 144–154.
[26] .
[27] X. Rios, P. Moriones, J.C. Echeverria, A. Luquin, M. Laguna, J.J. Garrido, Adsorption 17 (2011) 583–593.